Theoretical Investigation of the Mechanism of Methanol Carbonylation Catalyzed by Dicarbonyldiiodorhodium Complex

E. A. IVANOVA,[1] V. A. NASLUZOV,[1] A. I. RUBAYLO[1] and N. RÖSCH[2]

[1]*Institute of Chemistry and Chemical Technology, Siberian Branch of the Russian Academy of Sciences, Ul. K. Marxa 42, Krasnoyarsk 660049 (Russia)*

E-mail: ei@krsk.info

[2]*Institut für Physikalische und Theoretische Chemie, Technische Universität München, 85747 Garching (Germany)*

E-mail: roesch@ch.tum.de

Abstract

The entire potential energy profile of the catalytic cycle of methanol carbonylation catalyzed by $[Rh(CO)_2I_2]^-$ complex was explored computationally using a gradient-corrected density functional method and polarizable continuum model for accounting of solvent effects. For this purpose, the relative energies of the intermediates and transition states for CH_3I oxidative addition, the CO migratory insertion and the CH_3COI reductive elimination were estimated. Based on calculated energies the lowest-energy reaction path was deduced to be determined by the *cis*-dicarbonyl species in spite the *trans*-conformers of 6-coordinated intermediates $[RhCH_3(CO)_2I_3]^-$ and $[Rh(CH_3CO)(CO)_2I_3]^-$ were found to be more stable. The explanation is the lower activation barriers for transformation of *cis*-conformers to products. The activation barriers for oxidative addition, CO migratory insertion and reductive elimination steps were calculated to be at 135, 40 and 75 kJ/mol, respectively. The first step was found to be the rate-determining. The accounting for solvent effects makes the energy profile smoother and more consistent with experimental reaction profile.

INTRODUCTION

The catalytic carbonylation of methanol is one of the most efficient industrial method to produce acetic acid. Although this process has been discovered more than 35 years ago it still attracts attention of scientists. The catalytic process was a subject of numerous experimental studies [1–4] but the theoretical investigations are restricted to several investigations [5–7].

The catalytic cycle (Fig. 1) was proposed to consist of four main steps based on structures of intermediates as identified by X-ray crystallographic, IR and NMR spectroscopic data. The initial catalytically active species were found to be anionic complex $[Rh(CO)_2I_2]^-$ (**a** on Fig. 1). Its interaction with methyl iodide results in formation of kinetically unstable six-coordinated species $[Rh(CO)_2I_3CH_3]^-$ (**b**) imme-

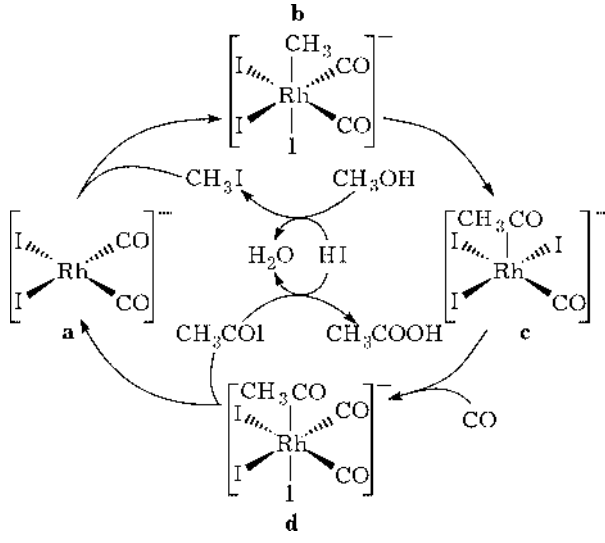

Fig. 1. Catalytic cycle of methanol carbonylation to acetic acid. Adapted from Ref. [4].

diately transformed into the isomeric five-coordinated acetyl complex $[Rh(CO)I_3(CH_3CO)]^-$ (**c**) as a result of the migration of methyl group to CO ligand. The latter reacts rapidly with carbon monoxide to give six-fold dicarbonyl acetyl complex $[Rh(CO)_2I_3(CH_3CO)]^-$ (**d**). Elimination of acetyliodide from the complex **d** finalizes the catalytic cycle and results in regeneration of initial active species **a**.

The knowledge about the mechanism of methanol carbonylation is deduced from the experiment based mainly on spectroscopic measurements. The latter can give information only on the kinetically stable and dominant species presented in reaction medium while short-lived unstable intermediates remain undetected and their role in catalytic process is unknown. The theoretical study, from other hand, can operate with different model species and provide helpful information unreachable with experimental technique.

On the other hand, methanol carbonylation reaction represents the ideal object for validating theoretical model. The activation energies and reaction heats for almost all elementary reaction steps are experimentally determined allowing the direct comparison of calculated and measured values. The other pecularity of this cycle is its reality. The same ligands as were used in industrial process are considered in our study. This is a significant improvement over a number of previous theoretical studies of catalytic cycles where large real groups were replaced with model ligands.

In this study we present systematic density functional study of the whole cycle of methanol carbonylation catalyzed by dicarbonyldiiodorhodium (I) complex. The points we want to address is the mechanism – backside or front-side – of the CH_3I oxidative addition – rate-determining step of the catalytic cycle. The influence of ligand arrangement on the activation barriers of CO migratory insertion and CH_3COI reductive elimination steps is of interest. The investigation of contribution of solvent effects in overall reaction profile is motivated because all the participants of catalytic cycle are charged species and are expected to be affected by solvent environment.

COMPUTATIONAL DETAILS

Density functional calculations were performed with the program suite Gaussian98 [8]. The geometries of all of intermediates as well as the corresponding transition states were optimized. D_{2h} and C_{2v} symmetry constraints were imposed for the *trans*- and *cis*-isomers of the 4-coordinated complex **a**, respectively. All other species **b**, **c**, and **d** were optimized with C_s symmetry constraints. No symmetry restrictions were applied during transition state searches.

We employed the gradient-corrected exchange functional proposed by Becke [9] in combination with the gradient-corrected correlation functional of Perdew [10] (BP86); all Kohn-Sham calculations were performed in spin-restricted fashion. For the heavy elements Rh and I, Hay-Wadt effective core potentials [11, 12] (in combination with standard double-ζ basis sets, LANL2DZ) were used to replace the core electrons up to 3*d*. The first-row elements were described by 6-311G(*d*,*p*) basis sets. To obtain more accurate energy estimates, an extended basis set was applied in single-point fashion at the previously optimized geometries. This extended basis set was decontracted [13] at the Rh center and augmented by one Rh *f*-type polarization exponent [14]. In the following we will only discuss the energetics calculated with the extended basis set.

Changes of the Gibbs free reaction energy $\Delta G(X \rightarrow Y)$ in the gas phase were calculated by taking zero-point energies, thermal motion, and entropy contributions at standard conditions (temperature 298.15 K, pressure 1 atm) into account. Solvent effects were estimated by employing the integral equation formalism of the polarizable continuum model [15]. Environment effects were estimated for dichloromethane CH_2Cl_2 (dielectric constant $\varepsilon = 8.9$ measured at 25 °C), one of the experimentally used solvents.

RESULTS AND DISCUSSION

In the following sections, we will describe the mechanism of each elementary step of the catalytic cycle separately starting from the structure and relative energies of reactants for

each step. Then discussion on the structures and activation energies of the corresponding transition states will be given. (The transition states are denoted by both corresponding reactant and product configurations. Also, we will refer to the two types of transition states for the methyliodide oxidative addition as "front" and "back".) Finally, we will discuss solvent effect and construct a free energy profile of the entire catalytic cycle.

Oxidative addition

The interaction of CH_3I with the planar complex **a** starts the catalytic cycle. This initial complex **a** has *cis*- and *trans*-isomers, denoted as **a1** and **a2**. Isomer **a1** with *cis*-carbonyl groups is more stable than the corresponding *trans*-isomer **a2** by 38 kJ/mol. The accounting for entropy does not change the relative energies; difference in free energies between to isomers is 39 kJ/mol. The larger stability of *cis*-isomer can be explained by the more effective bonding of carbonyl groups in **a1** (Rh–C bonds are shorter in **a1** than in **a2** on 0.06 Å). The domination of **a1** complex over **a2** is in agreement with experiment in which the initial catalytically active complex has been characterized as *cis*-isomer [2].

We have performed the comparative study of two possible mechanisms of CH_3I addition to rhodium complex. The first one is two-step "back-side" mechanism proceeded as classical S_N2 attack of rhodium center by methyliodide. The alternative one is single-step addition of methyliodide in "front-side" fashion. The investigation of S_N2 oxidative addition to the square planar $[Rh(CO)_2I_2]^-$ was carried out with special care. Since this mechanism involves the expulsion of an anion, I^-, the process is known to be difficult to describe by common density functional methods [16]. To reduce the effect of charge separation, NH_4^+ was introduced as model counter ion to accept the leaving iodide group; cations NBu_4^+ were used in the experiment. To be able to compare the relative energies of the transition states for two different mechanisms the transition state for "front-side" addition of methyliodide was also studied with accounting for ammonium counter ion. In our work we present only the results on CH_3I addition to complex **a1**; we refrained from considering the reactions of the less stable complex **a2**.

In **TS(a1-b1)$_{back}$** the Rh center of the complex $[Rh(CO)_2I_2]^-$ is attacked by the carbon of methyl iodide with the iodide atom turned away from the plane of the complex. CH_3I approaches the plane of the metal complex at an angle I1–C1–Rh of 140°; the CH_3 moiety is almost planar. In contrast, the alternative transition state **TS(a1-b1)$_{front}$** corresponding to "front-side" approach of substrate has a trigonal bipyramidal structure and can be considered as η^2-adduct of a butterfly-shaped fragment $[Rh(CO)_2I_2]^-$ and a methyliodide with an elongated C–I bond. Different orientation of substrate CH_3I molecule with respect to the plane of rhodium complex reflects in differences in activation parameters. The transition state **TS(a1-b1)$_{front}$** has an activation energy of 158 kJ/mol and free activation energy 195 kJ/mol (Table 1). The barrier of the transition state for the back-side attack of CH_3I, **TS(a1-b1)$_{back}$**, was estimated as 146 kJ/mol which increased to 189 kJ/mol after inclusion of entropy contribution. Thus, the activation energy of **TS(a1-b1)$_{back}$** in gas phase is by 6 kJ/mol lower than that of the corresponding front-side attack, **TS(a1-b3)$_{front}$**. The differentiation is further enhanced after accounting for solvent effects of reaction CH_2Cl_2 medium; activation free energy of **TS(a1-b1)$_{back}$** lowered to 135 kJ/mol while that for **TS(a1-b3)$_{front}$** reduced only slightly to 194 kJ/mol. The free activation barrier for **TS(a1-b1)$_{back}$** is 35 kJ/mol overestimated compared to the experimentally measured free activation energy for CH_3I oxidative addition to $[Rh(CO)_2I_2]^-$ at 100 kJ/mol. Thus, for the gas phase as well as for solution we confirm the preference of the back-side mechanism of CH_3I oxidative addition as it was previously reported.

The oxidative addition reaction is exothermic in the gas phase; although both products **b1** and **b3** are by 25 and 23 kJ/mol more stable than the separate reactants, CH_3I and complex **a1**. The negative entropies for oxidative addition process make them by 24 and 25 kJ/mol less stable than initial reactants. The solvent effects further increase of the

TABLE 1

Free energies $\Delta G_{solv}(Y)$ of solvation of selected stationary points Y, reaction energies $\Delta E(X \rightarrow Y)$, and free reaction energies $\Delta G(X \rightarrow Y)$ in the gas phase and estimates of the free reaction energies $\Delta G_{final}(X \rightarrow Y)$ in dichloromethane. All quantities (in kJ/mol) are calculated with the extended basis set

X	Y	$\Delta E(X \rightarrow Y)$	$\Delta G(X \rightarrow Y)$	$\Delta G_{solv}(Y)$	$\Delta G_{final}(X \rightarrow Y)$
	a1(NH_4)			−31.1	
a1(NH_4)[a]	**TS(a1-b1)$_{back}$**	146.0	188.7	−94.4	134.8
a1(NH_4)[a]	**TS(a1-b1)$_{front}$**	157.6	195.3	−42.0	193.8
a1	**a2**	37.5	39.4	−138.0	39.3
a1	**b1**	−25.4	23.6	−129.2	41.9
a2[a]	**b2**	−68.4	−18.8	−127.6	1.0
a1[a]	**b3**	−22.7	25.0	−125.9	46.5
a2[a]	**b3**	−60.2	−14.4		7.2
b1	**TS(b1-c)**	75.5	76.5	−131.1	74.5
b2	**TS(b2-c)**	81.0	80.1	−130.5	77.2
b3	**TS(b3-c)**	40.2	43.8	−127.8	42.0
b1	**c**	−37.4	−29.2	−130.8	−30.7
b2	**c**	−31.8	−26.0		−29.1
b3	**c**	−40.1	−30.6		−35.4
c[b]	**d1**	−59.4	−14.9	−124.5	−8.9
c[b]	**d2**	−64.8	−17.5	−124.2	−11.2
c[b]	**d3**	−39.3	6.4	−122.0	14.8
d1	**TS(d1-a1)**	72.7	74.2	−123.7	75.0
d2	**TS(d2-a2)**	89.3	81.8	−96.3	109.7
d3	**TS(d3-a1)**	79.6	77.7	−126.5	73.3
d1	**a1**[c]	48.8	−0.7	−138.0	−27.3
d2	**a2**[c]	91.6	41.3		14.5
d3	**a2**[c]	66.2	17.5		−11.5
d3	**a1**[c]	28.7	−21.9		−50.9
a1[d]	**a1**[c]	−73.4	−21.1		−24.9

[a]Energy of free CH_3I added to that of complexes **a**.
[b]Energy of free CO was added to that of complex **c**.
[c]Energy of free CH_3COI added to that of complexes **a**.
[d]Energy of free CH_3I and CO added to that of **a1.**
Note. The free energies of solution for CH_3I, CO and CH_3COI are −9.5, 0.3 and −13.0 kJ/mol, respectively.

product energies to 42 and 47 kJ/mol. The calculated free reaction energy is about 30 kJ/mol higher compared to those obtained in experiment (14 kJ/mol).

CO insertion

Migratory CO insertion takes place in sixfold methyl rhodium $[Rh(CO)_2I_3CH_3]^-$ complex to produce five-coordinated acetyl $[Rh(CO)I_3(CH_3CO)]^-$ complex. First, we have studied the relative energies of reactant **b** and its isomers. There are three isomeric structures of **b**: with both CO groups *cis* to each other and to methyl ligand (**b1**), with CO groups *trans* to each other (**b2**) and with CO groups *cis* to each other and one carbonyl ligand *trans* to methyl group (**b3**). All the isomers were calculated to have similar energies with **b2** complex being the most stable and **b1** and **b3** complexes are by 6 and 8 kJ/mol higher in energy, respectively. The relative energies of **b1** and **b3** with respect to **b2** corrected for entropy are by 3 and 4 kJ/mol, correspondingly. The lowest stability of **b3** structure can be explained by the presence of carbonyl CO group with strong *trans*-influence in *trans*-position to methyl group and as a consequence weakening of $Rh-CH_3$ bond. Preference of *trans*-isomer **b2** over *cis*-isomer **b1** can be rationalized in

terms of larger overlap of rhodium d_z^2-orbital with carbon orbital of methyl group in **b2**. The decreasing of the overlap in **b1** is due to tilting of methyl group towards CO groups induced by the electrostatic repulsion from iodides.

From NMR and IR data, the intermediate formed after CH_3I oxidative addition to the square-planar complex **a** was deduced to be isomer **b1**. In NMR, only one doublet was observed in the rhodium carbonyl region, indicative of equivalent carbonyl ligands, as in **b1** and **b2**. In the IR spectrum, two carbonyl bands were found to have similar intensities, as expected for the *cis* dicarbonyl species **b1**. However, the spectroscopic data reported in Ref. do not provide direct information on the number of iodide ligands in complex **b**. Alternative structures of the observed intermediate are the neutral five-coordinated species $[Rh(CO)_2I_2CH_3]^-$ or, more likely in solution, a neutral solvent complex $[Rh(CO)_2I_2CH_3(solvent)]$. Yet another rationalization of the observation of complex **b1** instead of the more stable isomer **b2** can be proposed. Complex **b2** forms after addition of CH_3I to **a2**, but the lower stability of the latter complex compared to **a1** prevents the reaction **a2** $\rightarrow$ **b2**. Thus, initial formation of **b1** by addition of CH_3I to **a1** is favored. In the next step, the rearrangement **b2** $\rightarrow$ **c** by CO migration exhibits a higher barrier than the analogous processes **b1** $\rightarrow$ **c** and **b3** $\rightarrow$ **c** (see discussion on transition states energies below). Thus, in the overall dynamics, **b2** isomerizes to **b1** or **b3** to permit a reaction path with a lower barrier for CO migration. Thus, complex **b2** is not observed because of fast conversion to other isomers and small concentration. Therefore, to arrive at a description consistent with available experimental information, it is necessary to estimate activation energy barriers for the various elementary steps.

Since three isomeric forms are possible for species **b**, three reaction paths corresponding to the transformations of methyl complexes to acetyl ones has been investigated. All three transition states involve rearrangements of three centers, they have trigonal bipyramidal structure with CH_3 group shifted towards neighboring carbonyl group. The calculated activation barriers for CO insertion in **b1**, **b2** and **b3** complexes are 76, 81 and 40 kJ/mol, respectively. The corresponding free energy barriers are 77, 80 and 44 kJ/mol. The experimentally observed activation energy at 81 kJ/mol corresponds to either **TS(b1-c)** or **TS(b2-c)** structure while **TS(b3-c)** is not observed probably because of the low concentration of **b3** complex. The smallest barrier for **TS(b3-c)** may be rationalized by the observation that in **TS(b3-c)** a strong *trans*-effect of CO facilitates the stretching and breaking of $Rh-CH_3$ bond in *trans*-position, thus reducing the activation barrier of this TS. In the other two transition states, an iodide is in *trans*-position to the migrating CH_3 group, which decreases the activation barrier less, due to a weaker *trans*-influence. Since the activation parameters for **TS(b1-c)** with iodide in *trans*-position to forming acetyl group and for **TS(b2-c)** with CO *trans* to acetyl ligand are close within few kilojoules the effect of ligand in position *trans* to CH_3CO group is very minor.

The CO insertion step is exothermic with calculated reaction energies −37, −32 and −40 kJ/mol for paths started from **b1**, **b2** and **b3** complexes, respectively. The corresponding free energies are −29, −26 and −31 kJ/mol. Solvent effect contribution into reaction energies does not exceed 5 kJ/mol. The calculated values agrees quite well with experimental enthalpy and free energy measured at −36 and −20 kJ/mol.

Reductive elimination

By uptake of a CO ligand into the free octahedral coordination site, complex **c** transforms into **d** species, the precursor complex for reductive elimination. During this step, a comparatively strong bond is formed and no bonds are broken; therefore, we refrained from studying transition structures. In fact, the reaction is quite exothermic with reaction energies of −59, −65, and −39 kJ/mol for the reactions **c** $\rightarrow$ **d1**, **c** $\rightarrow$ **d2**, and **c** $\rightarrow$ **d3**, respectively (see Table 1).

The last elementary step of the catalytic cycle (see Fig. 1) is the reductive elimination of acetyliodide from the octahedral complex **d**. Similarly to the complexes **b** the acetyl species **d** posses three isomeric conformations. The order of stability for complexes **d** agrees with

that for complexes **b**. The isomer **d2** was calculated to be more stable than **d1** and **d3** conformers by 5 and 26 kJ/mol, respectively. Inclusion of entropy and solvent effects does not change the trend in stability of the isomers and weakly affects their relative energies.

We have considered three different routes for the transformation of **d**-type species into isomers of complex **a**. Transition states **TS(d1-a1)** and **TS(d3-a1)** have trigonal bipyramidal structures and can be viewed as η^2-adducts of the butterfly shaped fragment $Rh(CO)_2I_2$ and an elongated carbon-iodine σ-bond of CH_3COI fragment. On the other hand, the **TS(d2-a2)** features almost planar fragment $Rh(CO)_2I_2$, which interacts with acetyliodide only by coordination of the carbonyl carbon to the rhodium center; iodine is significantly transferred to the acetyl fragment. The activation energies of the three transition states **TS(d1-a1)**, **TS(d2-a2)**, and **TS(d3-a1)** for reductive elimination are 73, 89 and 80 kJ/mol, respectively (see Table 1). The corrected for entropy contribution these barriers are 74, 82 and 78 kJ/mol, correspondingly. Accounting for solvent effects increase of the activation energy of **TS(d2-a2)** to 110 kJ/mol and remains unchangable barriers of **TS(d1-a1)** and **TS(d3-a1)**. The activation barriers for transition states of reductive elimination process can be rationalized in terms of ligand *trans*-influence located in *trans*-position to the eliminated acetyl and iodide groups. Indeed, the structure, **TS(d2-a2)**, with two iodide ligands possessing weaker *trans*-effect located in *trans* to leaving groups has the higher energy than the structures with carbonyl and iodide ligands in *trans*-position to eliminating groups.

Reductive elimination of acetyliodide was found to be endothermic with reaction energies of 49, 29, 66, and 92 kJ/mol for the paths **d1** → **a1**, **d3** → **a1**, **d3** → **a2** and **d2** → **a2**, respectively. Positive values of entropy for acetyliodide elimination process as well as solvent effect make the decomposition of complexes **d** exothermic reaction.

Entire profile

Following to the lowest-free-energy transition states of elementary steps the most favorable free energy profile can be extracted (Fig. 2). As one can see the oxidative addition step has the highest activation barrier in the gas-phase. The barriers for migratory insertion and reductive elimination steps are much more modest. Accounting for solvent effects makes the shape of potential energy profile smoother. Solvent effects significantly reduce the barrier associated with transition state for oxidative addition and increase the energies corresponding to the intermediates and transition states for three consequent steps. It should be mentioned that the minimal potential energy

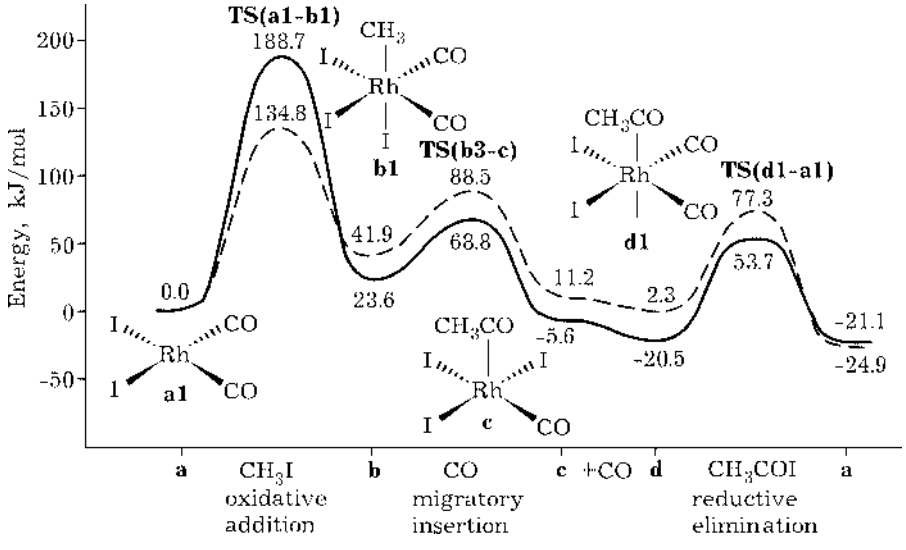

Fig. 2. Calculated free energy profile of methanol carbonylation catalytic cycle in the gas phase (solid line) and in solution (dashed line).

profile is determined by *cis*-dicarbonyl isomers of intermediate complexes **a1**, **b1** and **d1** while the *trans*-conformers for complexes **b** and **d** are calculated to be more stable. The reason is higher activation barriers associated with transformation of *trans*-species to products. The preference of *trans*-intermediates as well as high barriers for their transformation can be explained in terms of ligand *trans*-influence. It was found that the factors favored the stability of *trans*-intermediates become unfavorable for transformation of corresponding complexes to the products.

CONCLUSIONS

We have carried out a density functional study of the full methanol carbonylation cycle catalyzed by the rhodium complex $[Rh(CO)_2I_2]^-$. To our best knowledge this is the first systematic investigation of this reaction in frameworks of unique theoretical approach with accounting for entropy and solvent effects on each elementary step. We have investigated the molecular structures of various catalytically active intermediates involved in methanol carbonylation cycle as developed by Forster (see Fig. 1): the complexes **a** $[Rh(CO)_2I_2]^-$, **b** $[RhCH_3(CO)_2I_3]^-$, **c** $[Rh(CH_3CO)(CO)I_3]^-$, and **d** $[Rh(CH_3CO)(CO)_2I_3]^-$.

The preference for the *cis*-conformation of complex **a** and the *trans*-conformation of complex **d** found in the present work are in agreement with available experimental data. In contrast to the interpretation of experimental data, the calculations showed complex **b** to be most stable in the *trans*-conformation.

We were able to locate the transition states of three elementary reaction steps. These computational results corroborate that the rate-determining step of the methanol carbonylation is the CH_3I oxidative addition reaction with a calculated activation barrier 135 kJ/mol. The activation barrier of the CO migratory insertion **b** → **c** and final CH_3COI reductive elimination step **d** → **a** was calculated to be 40 and 75 kJ/mol, *i. e.* lower than that of the CH_3I oxidative addition step **a** → **b**.

Solvent effects were found to be of crucial importance for estimating the barrier of the rate determining step **a** → **b** and, thus, for delineating the overall reaction profile. In general, the accounting for solvent effects improve the correspondence between calculated and experimental energy profiles.

Based on the calculated reaction energies and activation barriers of the elementary steps of the catalytic cycle, we proposed the reaction path **a1** → **b1** → **b3** → **c** → **d1** → **a1** as most favorable for methanol carbonylation (see Fig. 2).

Acknowledgements

The authors thank Volkswagen Foundation (grant No. I/73 653), INTAS-RFBR (grant No. IR–97–1071, RFBR No. 97–03–71057) and scientific program "University of Russia" (grant No. UR.05.01.032) for financial support.

REFERENCES

1 D. Forster, *J. Am. Chem. Soc.*, 98 (1977) 846.
2 D. Forster, *Adv. Organomet. Chem.*, 17 (1979) 255.
3 L. A. Howe and E. E. Bunel, *Polyhedron*, 14 (1995) 167.
4 A. Haynes, B. E. Mann, G. E. Morris and P. M. Maitlis, *J. Am. Chem. Soc.*, 115 (1993) 4093.
5 T. R. Griffin, D. B. Cook, A. Haynes *et al., Ibid.*, 118 (1996) 3029.
6 M. Cheong, R. Schmid and T. Ziegler, *Organometallics*, 19 (2000) 1973.
7 E. A. Ivanova, Ph. Gisdakis, V. A. Nasluzov *et al., Ibid.*, 20 (2001) 1161.
8 M. J. Frisch, G. W. Trucks, H. B. Schlegel *et al.*, Gaussian 98, Revision A.3; Gaussian, Inc., Pittsburgh PA, 1998.
9 A. D. Becke, *Phys. Rev. A.*, 38 (1988) 3098.
10 J. P. Perdew, *Phys. Rev. B.*, 33 (1986) 8822.
11 W. R. Wadt and P. J. Hay, *J. Chem Phys.*, 8 (1985) 284.
12 W. R. Wadt and P. J. Hay, *Ibid.*, 82 (1985) 299.
13 G. Frenking, I. Antes, M. Böhme *et al.*, in K. B. Lipkowitz, D. B. Boyd (Eds.), Reviews in Computational Chemistry, vol. 8, VCH, New York, 1996, p. 63.
14 A. W. Ehlers, M. Böhme, S. Dapprich *et al., Chem. Phys. Lett.*, 208 (1993) 111.
15 C. Amovili, V. Barone, R. Cammi *et al., Adv. Quantum. Chem.*, 32 (1999) 227.
16 N. Rösch, S. B. Trickey, *J. Chem. Phys.*, 106, 21 (1996) 8940.